

QUASI FREE $^{238}\text{U}(e, e'f)$ -CROSS SECTION IN MACROSCOPIC-MICROSCOPIC APPROACH

V. P. Likhachev^a J. Mesa^{a,b} J. D. T. Arruda-Neto^{a,c}, B. V. Carlson^d, W.R. Carvalho^a Jr,
L.C. Chamon^a, M.T.F.da Cruz^a, A. Deppman^a, H. Dias^a, M. S. Hussein^a

^a *Instituto de Física, Universidade de São Paulo, São Paulo, Brazil.*

^b *Instituto Superior de Ciencias y Tecnologia Nucleares, Havana, Cuba.*

^c *Universidade de Santo Amaro, Sao Paulo, Brazil.*

^d *Instituto de Estudos Avançados-Centro Técnico Aeroespacial, São José dos Campos, Brazil.*

Abstract

We present the result of a theoretical study of inclusive quasi free electrofission of ^{238}U . The off-shell cross sections for the quasi free reaction stage have been calculated within the Plane Wave Impulse Approximation (PWIA), using a Macroscopic -Microscopic description of the proton and neutron single particle momentum distributions. Electron wave function distortion corrections were included using the effective momentum approximation, and the Final State Interaction (FSI) effects were calculated using an optical potential. The fissility for the proton single hole excited states of the residual nucleus ^{237}Pa was calculated both without and with contributions of the pre-equilibrium emission of the particles. The fissility for $^{237,238}\text{U}$ residual nuclei was calculated within the compound nucleus model. The $(e, e'f)$ -cross sections thus obtained were compared with available experimental data.

I. INTRODUCTION

A new aspect of investigations of quasi free scattering of high energy electrons (QF) has been opened with the study of decay channels of single hole states in the residual nucleus, created as a result of the QF process. Especially interesting is to study fission following a QF process. In this case we have an essentially single particle process in the first reaction stage, and an essentially collective process in the final reaction stage. The collective degrees of freedom are excited in the intermediate reaction stage due to the residual interaction.

This is a new kind of nuclear reaction which may allow to get unique information on the dissociation of well defined single hole configurations (which we can select by coincidence ($e, e'p$)) into complex nuclear configurations, and its role in nuclear fission. In particular, to study the limitations associated with the predictions of the shell model based on the mean field approximation and residual forces for heavy nuclei such as ^{238}U .

The new and most important aspect of this reaction is that, after knocking-out a proton or neutron, we obtain the heavy residual nucleus ^{237}Pa or ^{237}U in a single hole doorway state (see discussion below), which could undergo nuclear fission. Indeed, instead of dealing with collective doorway states, which are coherent sums of a great number of 1p-1h configurations (a common situation, well-known giant resonances), these non-collective doorway states will be represented by only one, well defined, 1h configurations. The residual interaction mixes these 1h configurations with more complicated 2h-1p and 3h-2p ones and fission may occur either directly from 1h configurations, or, with some delay, from the mixed states (or their components). Since in the case of QF we have in the initial state only one configuration, the fission probability P_f should be more sensitive to the individual structure of this initial state as compared with conventional reactions, where the effects of the structure are averaged out over many single particle states forming the doorway. The specific features of the quasi free reaction $^{238}\text{U} (e, e'pf)$ may create a new situation when some of the single hole levels, which coincide in energy position and quantum numbers with the collective levels in the second well, have their fission probability enhanced and thus, the dependence on state structure

should be favored, which is also a rather unusual and non-trivial situation.

The unambiguous extraction of single hole contributions is possible only in an exclusive experimental scheme (reaction $(e, e' pf)$) This kind of experiment involves extremely thin targets (fission fragments have to leave the target with small energy losses), high energy resolution and coincidence between the final particles (to separate the single hole states) and has never been performed. The advent of high energy CW electron accelerators, combined with the development of high resolution facilities, opens the possibility of studying the fission channel for quasi free electron scattering in an exclusive experimental setup. The most suitable accelerator for this experiment is at the Thomas Jefferson National Accelerator Facility (TJNAF).

Some integral properties of the quasi free electrofission could be studied in inclusive experiments: (e, f) [1] and $(e, e' f)$ [2]. These works dealt only with the total issue of the QF contribution in electrofission.

The goal of the present work is the calculation of the quasi free $(e, e' f)$ -differential cross section for ^{238}U , based on the macroscopic-microscopic approach for the description of the quasi free reaction stage, and the statistical theory for an estimate of the fissility for single hole states in the residual nucleus. The comparison with available inclusive experimental data will serve to check the models used for the description of quasi free fission for heavy deformed nuclei.

II. PWIA SIX-FOLD DIFFERENTIAL CROSS SECTION

In the first order Born approximation, the electron with initial four-momentum $k_{1\mu} = (\vec{k}_1, i\varepsilon_1)$ and final four-momentum $k_{2\mu} = (\vec{k}_2, i\varepsilon_2)$ interacts with the target nucleus and transfers a virtual photon with four-momentum $q_\mu = (\vec{q}, i\omega) = k_{1\mu} - k_{2\mu}$, leading to a final state with a knocked-out nucleon with $p_\mu = (\vec{p}, iE)$ and a residual nucleus with $P_{A-1\mu} = (\vec{P}_{A-1}, iE_{A-1})$.

In the impulse approximation, a virtual photon interacts with a bound nucleon (proton or

neutron) of four-momentum $p_m = (\vec{p}_m, iE_m)$, which exits the nucleus with four-momentum $p_\mu = (\vec{p}, iE)$ without further interaction (no FSI). In the PWIA approximation $\vec{p}_m = -\vec{P}_{A-1}$ and the missing quantities (momentum and energy of the nucleon before interaction) can be defined from the energy and momentum conservation law in the following way:

$$\vec{p}_m = \vec{p} - \vec{q}, \quad (1)$$

$$E_m = \omega - T - T_{A-1},$$

where $E_m = M_{A-1} + m - M_A$ is the nucleon missing (or separation) energy, T is the kinetic energy of the outgoing nucleon, and T_{A-1} is the kinetic energy of the residual nucleus. The momentum and energy of the virtual photon can be varied independently.

In the plane wave impulse approximation (PWIA) the six-fold differential cross section of the $(e, e'p)$ - reaction in the Laboratory system has the following form [3]:

$$\frac{d^6\sigma}{d\Omega_e d\Omega_N d\varepsilon_2 dE} = pE\sigma_{eN}S(E_m, \vec{p}_m), \quad (2)$$

where

$$\sigma_{eN} = \sigma_{mott} (V_C W_C + V_T W_T + V_I W_I + V_S W_S) \quad (3)$$

is the off-shell electron-nucleon cross section, and $S(E_m, \vec{p}_m)$ is the spectral function which defines the combined probability to find a bound nucleon with momentum \vec{p}_m on the shell with separation energy E_m .

The kinematic functions V in Eq. (3) can be expressed, neglecting the mass of the electron, in the following way:

$$V_C = \frac{q_\mu^4}{q^4}, \quad (4)$$

$$V_T = \frac{q_\mu^2}{2q^2} + \tan^2\left(\frac{\theta_e}{2}\right), \quad (5)$$

$$V_I = \frac{q_\mu^2}{q^2} \cos \phi \sqrt{\frac{q_\mu^2}{q^2} + \tan^2\left(\frac{\theta_e}{2}\right)}, \quad (6)$$

$$V_S = \frac{q_\mu^2}{q^2} \cos^2 \phi + \tan^2\left(\frac{\theta_e}{2}\right), \quad (7)$$

and

$$\sigma_{mott} = \frac{\alpha^2 \cos^2 \frac{\theta_e}{2}}{4\varepsilon_1^2 \sin^4 \frac{\theta_e}{2}} \left(1 + \frac{2\varepsilon_1}{m_p} \sin^2 \frac{\theta_e}{2}\right)^{-1}.$$

Above, σ_{mott} is the Mott cross section, θ_e is the electron scattering angle, and ϕ is the angle between the scattering plane and the plane defined by the vectors \vec{p} and \vec{q} , $\alpha = 1/137$ is the fine structure constant.

For the structure functions W in Eq.(3) we use the off-shell prescription of de Forest [3]:

$$\begin{aligned} W_C &= \frac{1}{4\bar{E}E} \{(\bar{E} + E)^2(F_1^2 + \frac{\bar{q}_\mu^2}{4m^2}\kappa^2 F_2^2) - q^2(F_1 + \kappa F_2)^2\}, \\ W_T &= \frac{\bar{q}_\mu^2}{2\bar{E}E} (F_1 + \kappa F_2)^2, \\ W_I &= -\frac{p \sin \gamma}{\bar{E}E} (\bar{E} + E)(F_1^2 + \frac{\bar{q}_\mu^2}{4m^2}\kappa^2 F_2^2), \\ W_S &= \frac{p^2 \sin^2 \gamma}{\bar{E}E} (F_1^2 + \frac{\bar{q}_\mu^2}{4m^2}\kappa^2 F_2^2), \end{aligned} \quad (8)$$

where κ is the anomalous magnetic moment of the nucleon in units of the Bohr magneton ($\kappa_p = 1.793$, $\kappa_n = -1.913$),

$$\bar{E} = \sqrt{p_m^2 + m^2}, \quad (9)$$

m is the mass of the nucleon, $\bar{q}_\mu = (\vec{q}, i\bar{\omega})$, $\bar{\omega} = E - \bar{E}$, γ is the angle between \vec{p} and \vec{q} , and F_1 and F_2 are the on-shell Dirac and Pauli nucleon form factors, respectively.

$$F_1(q_\mu^2) = \frac{1}{1 + \frac{q_\mu^2}{4m^2}} [G_E(q_\mu^2) + \frac{q_\mu^2}{4m^2} G_M(q_\mu^2)], \quad (10)$$

$$\kappa_p F_2(q) = \frac{1}{1 + \frac{q_\mu^2}{4m^2}} [G_M(q_\mu^2) - G_E(q_\mu^2)], \quad (11)$$

where for protons

$$G_E^p(q_\mu^2) = \left(\frac{1}{1 + \frac{q_\mu^2}{0.71}} \right)^2, \quad (12)$$

$$G_M^p(q_\mu^2) = \mu_p G_E^p(q_\mu^2)], \quad (13)$$

and for neutrons

$$G_M^n(q_\mu^2) = \mu_n G_E^n(q_\mu^2)], \quad (14)$$

$$G_E^n(q_\mu^2) = |G_M^n(q_\mu^2)| \frac{q_\mu^2}{4m^2} \left(\frac{1}{1 + \frac{5.6q_\mu^2}{4m^2}} \right), \quad (15)$$

$\mu_p = 1 + \kappa_p = 2.793$ and $\mu_n = \kappa_n = -1.913$ are the proton and neutron magnetic moments in units of the Bohr magneton, respectively, and q_μ^2 in Eq.(12) is in $(\text{GeV}/c)^2$;

III. PWIA THREE-FOLD DIFFERENTIAL CROSS SECTION

In the independent particle shell model the spectral function for the spherical orbitals $\alpha \equiv nlj$ with binding energy E_α takes the simple form:

$$S(E_m, \vec{p}_m) = \delta(E - E_\alpha) v_\alpha^2 n_\alpha(\vec{p}_m), \quad (16)$$

where v_α^2 and $n_\alpha(\vec{p}_m)$ are the occupation number and momentum distribution of the α orbital, respectively. The six-fold $(e, e'p)$ -cross section could be transformed into a five-fold one:

$$\frac{d^5\sigma}{d\Omega_e d\Omega_N dE} = pE\sigma_{eN} v_\alpha^2 n_\alpha(\vec{p}_m), \quad (17)$$

where energy and momentum conservation are imposed for the kinematic variables that appear in σ_{eN}

To obtain the three-fold (e, e') -cross sections for each bound proton and neutron orbital we have integrated Eq.(17) over $d\Omega_N$ using a Monte Carlo approach. For each fixed ε_2 we calculate q neglecting the recoil energy of the residual nucleus:

$$q = \sqrt{k_1^2 + k_2^2 - 2k_1k_2 \cos \theta_e}, \quad (18)$$

and the kinetic energy of ejected nucleon:

$$T = \omega - E_\alpha. \quad (19)$$

Then, we generate randomly and uniformly the directions of the ejected nucleon with respect to \vec{q} and calculate the corresponding momentum of the internuclear nucleon p_m . Finally, using the values of v_α^2 and $n_\alpha(p_m)$ (see below) we calculate

$$\frac{d^5\sigma}{d\Omega_e d\Omega_N d\varepsilon_2}(p_m) \quad (20)$$

The three-fold (e, e') -cross section was obtained as:

$$\frac{d^3\sigma}{d\Omega_e d\varepsilon_2}(\varepsilon_2) = \langle \frac{d^5\sigma}{d\Omega_e d\Omega_N d\varepsilon_2} \rangle > 4\pi \quad (21)$$

where the average five-fold cross section is

$$\langle \frac{d^5\sigma}{d\Omega_e d\Omega_N d\varepsilon_2} \rangle = \frac{\sum \frac{d^5\sigma}{d\Omega_e d\Omega_N d\varepsilon_2}}{N}, \quad (22)$$

and N is the number of Monte Carlo starts

IV. SINGLE PARTICLE BOUND STATES

The single particle bound state energies and momentum distributions were calculated in the framework of the macroscopic-microscopic approach using the BARRIER code [4].

The energy of the nucleus is given as:

$$E_{tot} = E_{LD} + \delta E_{shell}, \quad (23)$$

where E_{LD} is the macroscopic liquid drop part of the energy and δE_{shell} is the shell correction, which describes the shell and pairing effects. Both shell correction and the macroscopic part of the energy have been calculated according to [4].

Axially symmetric nuclear shapes have been considered in the present work, and from these potential energy surfaces, the equilibrium (ground state) deformation parameters ε (elongation) and α_4 (hexadecapolar momentum) have been calculated by minimizing the total nuclear energy (Eq.(23)), obtaining thus, $\varepsilon = 0.227$ and $\alpha_4 = 0.059$.

An Woods- Saxon potential [5] consisting of a central part V , spin-orbit part V_{SO} , and Coulomb part V_{Coul} for protons was employed:

$$V^{WS}(r, z, \varepsilon, \hat{\alpha}) = V(r, z, \varepsilon, \hat{\alpha}) + V_{so}(r, z, \varepsilon, \hat{\alpha}) + V_{Coul}(r, z, \varepsilon, \hat{\alpha}) \quad (24)$$

The real potential $V(r, z, \varepsilon, \hat{\alpha})$ involves the parameters V_0 , r_0 and a , describing the depth, radius and diffuseness of the central potential, respectively, and is expressed as:

$$V(r, z, \varepsilon, \hat{\alpha}) = \frac{V_0}{1 + \exp\left[\frac{dist(r, z, \varepsilon, \hat{\alpha})}{a}\right]}, \quad (25)$$

where $dist(r, z, \varepsilon, \hat{\alpha})$ is the distance between a point and the nuclear surface, and ε and $\hat{\alpha}$ are deformation parameters.

The depth of the central potential is parametrized as

$$V_0 = V_0[1 \pm \kappa(N - Z)/(N + Z)], \quad (26)$$

with the plus sign for protons and the minus sign for neutrons, with the constant $\kappa = 0.63$.

The spin-orbit interaction is then given by:

$$V_{so}(r, z, \varepsilon, \hat{\alpha}) = \lambda \left(\frac{\hbar}{2Mc} \right)^2 \nabla V(r, z, \varepsilon, \hat{\alpha}) \cdot (\vec{\sigma} \times \vec{p}), \quad (27)$$

where λ denotes the strength of the spin-orbit potential and M is the nucleon mass. The vector operator $\vec{\sigma}$ stands for Pauli matrices and \vec{p} is the linear momentum operator.

The Coulomb potential is assumed to be the one corresponding to the nuclear charge $(Z - 1)e$, uniformly distributed inside the nucleus.

For the ground state deformation of ^{238}U , small changes in λ (spin-orbit potential strength) and r_{0-so} (spin-orbit potential radius) of the Chepurnov parameters [7] are introduced in order to reproduce adequately the spin/parity of the levels sequence. Using single particle states obtained by this procedure, the quasiparticle states can be calculated for the first minimum region, providing spin, parity, energy and level spacing for the ground and some low-lying states. The quasiparticle spectrum was obtained by using the semi-microscopic combined method [8].

The potential parameters were chosen to give the best fit to the spectrum of single-quasiparticle excitations of the neighboring nuclei. The Hamiltonian matrix elements are

calculated with the wave functions of a deformed axially symmetric oscillator potential. The wave functions ϕ_i in the coordinate space are expanded into eigenfunctions of the axially deformed harmonic oscillator potential. From this expansion, we conveniently express the single particle Woods-Saxon wave function in momentum space. These single particle momentum distributions were averaged over the nuclear symmetry axis directions. The occupation probabilities were calculated in the framework of the BCS model [8]. The results for the occupation number calculations are shown in Fig. 1. Fig. 2 shows 6 typical averaged momentum distribution for proton bound states.

V. FISSION

The quasi free knockout of nucleons leads to the excitation of the residual nucleus ^{237}Pa , in the case of $(e, e'p)$ reaction, and ^{237}U for $(e, e'n)$. The excitation energy E^* (nucleus A-1) has two origins: holes in the shells of the nucleus A, which appear as a result of the knockout of nucleons, and final state interaction (FSI) of the outgoing nucleon.

The fast, quasi free reaction stage occurs at zero thermal excitation (ground state) of the initial nucleus ^{238}U , and results in a single hole in one of the shells. This single hole configuration forms a doorway for a thermalization process which leads to the thermal excitation E^* of the residual nucleus.

The thermalization is a complicate process which involves creation of new many particle-hole configurations in competition with particle emission and fission, and for some doorway configurations it might have non-statistical character, but, as a first guide-line for order of magnitude estimates we calculate the total fission probability (nucleus with energy E^* deexcites in several steps) using the statistical theory, both with and without taking into account the preequilibrium decay.

1. *Thermalization without preequilibrium decay.*

Firstly, we considered an extreme situation, by assuming that the residual interaction leads to thermalization and formation of compound nucleus just after the fast reaction stage, without any preequilibrium particle emission. In this case, the compound nucleus excitation energy is assumed to be :

$$E^* = -E_\alpha + E_f \quad (28)$$

where E_α and E_f are the energies of the bound state (hole) and Fermi level, respectively.

For the calculations of the compound nucleus fissility we used the Bohr-Wheeler [9] and Weisskopf [10] models for the description of the evaporation/fission competition. A Monte Carlo algorithm [11] was developed for the evaporation/fission process which includes not only the neutron evaporation vs fission competition, but also takes into account the proton and alpha-particle contributions.

The Monte Carlo code for Evaporation-Fission [12] calculates, at the i^{th} step of the evaporation chain, the fission probability F_i , and then chooses randomly which particle will evaporate (neutron, proton or alpha particle), according to their relative branching ratios. After evaporation, the mass, atomic number and excitation energy of the new residual nucleus are calculated. This process continues until the excitation energy available in the nucleus is not enough to emit any of the possible evaporating particles. At this point, the evaporation process stops, and we can calculate the nuclear fissility by the expression

$$W = \sum_i \left[\prod_{j=0}^{i-1} (1 - F_j) \right] F_i, \quad (29)$$

where

$$F_j = \frac{(\frac{\Gamma_f}{\Gamma_n})_i}{1 + (\frac{\Gamma_f}{\Gamma_n})_i + (\frac{\Gamma_p}{\Gamma_n})_i + (\frac{\Gamma_\alpha}{\Gamma_n})_i}, \quad (30)$$

$\Gamma_f, \Gamma_n, \Gamma_p, \Gamma_\alpha$ are fission, neutron, proton and alpha-particle decay widths, respectively.

The probability for the emission of a particle j is calculated within the Weisskopf statistical model [10]. The level density for the initial and final nucleus are calculated from the Fermi gas expression.

The fission barriers were taken as 6.13, 5.2 and 5.62 MeV and the neutron separation energies as 5.78, 5.12 and 5.04 MeV in the first step for ^{237}Pa , ^{237}U , and ^{238}U , respectively. These values reproduce the experimental data for P_f (see below).

For the other steps in the evaporation chain the fission barrier is calculated as [13],

$$B_f = C(0.22(A - Z) - 1.40Z + 101.5) \text{ MeV}, \quad (31)$$

where $C = 1 - \frac{E^*}{B}$ is the factor which take into account the dynamical effects [13], B is the total nuclear binding energy [13], and E^* is the nuclear excitation energy.

The neutron separation energy was taken from [14] for the other steps.

Using the model described above, we have calculated the fissility for ^{237}Pa , ^{237}U and ^{238}U (figure 3, solid curves). The peaks observed in the fissility correspond to the opening of the fission channel in the daughter nuclei. In figure 3 the experimental data for the fissility of ^{237}Pa , ^{237}U ([15]) and ^{238}U ([15], [2]) are also shown by dark strips. Data for ^{237}Pa were obtained by extrapolation of the neutron to fission width ratios for $Z = 91$ and $A = 230, 231, 232, 233$ [16] to $A = 237$, using the empirical trend presented in Vandenbosch and Huizenga [15].

It should be pointed out that in our calculations of the fissility we assumed that the hole excitation energies for an $A-1$ nucleus correspond to the compound nucleus excitation energies (see Eq. (28)), that is to say, complete thermalization is reached without any preequilibrium decay. Such calculations could be considered as upper limits for the fissility.

2. Account of the preequilibrium decay

The calculation of preequilibrium decay [17], [18] was performed only for ^{237}Pa , since the $(e, e'p)$ -reaction gives the main contribution to the total QF cross section. We used the exciton model [19], [20], [21] and the code STAPRE. In this model, the states of the system are classified according to the number of excitons n , which corresponds to the total number of excited particle p and hole h degrees of freedom, $n = p + h$. Starting from a simple

configuration of low exciton number, the system is assumed to equilibrate through a series of two-body collisions and to emit particles from all intermediate states. The application of a two-body interaction to states of a (p, h) configuration results in states with $(p + 1, h + 1)$, (p, h) , and $(p - 1, h - 1)$ excited particles and holes. The transition rates, which are taken to be averages over all states of a configuration, do depend on the number of excited particles and holes, and $\lambda_+(n)$ are the average rates for internal transitions from the n exciton configuration with a change of exciton number by -2, 0, or +2.

The decay is described using the Hauser-Feshbach formalism. We have considered fission in competition with neutron and gamma emission.

The initial configuration in ^{237}Pa , consistent with the proton knockout reaction for ^{238}U initiating the statistical cascade, consists of one-particle at the Fermi level and one-hole in a bound state. Our calculations were performed assuming only an one-hole initial configuration of the $l=0$ partial wave alone. The particle at the Fermi level contributes negligibly to the equilibration process. The fission barriers, neutron separation energies and level density parameters were taken to be the same as those of the compound nucleus calculations in the previous section.

The exciton model fissility results for single hole states of ^{237}Pa are shown in fig 3 by the dotted curve. We note that these calculations for fissility show a smoother behavior than that for the compound model. The preequilibrium particle emission removes some excitation energy before a equilibrium is reached reducing, therefore, the probability of opening new chances for fission.

VI. DISTORTION CORRECTIONS TO PWIA

An exact treatment of distortions of initial and final electrons and knocked-out nucleon waves, arising from the vicinity of a heavy nucleus, requires the solution of the Dirac equation for a large number of partial waves and is a hard special task. In the case of an inclusive

quasi free reaction, the distortion corrections are averaged over directions of ejected nucleon and we will treat these distortions qualitatively in an effective way.

The main effect of electron wave distortions, produced by the attractive Coulomb potential of a nucleus, could be treated as an effective increase of the momentum transfer (effective momentum approximation (EMA) [23]). For the calculation of q_{eff} we use the prescription of [24], namely

$$\vec{q}_{eff} = \vec{q} \left(1 + \frac{3Z\alpha}{2\varepsilon_1 R}\right) - \frac{3Z\alpha}{2\varepsilon_1 R} \omega \frac{\vec{k}_2}{k_2},$$

where $R = 1.2A^{1/3}$ is the equivalent nuclear radius. The account of the Coulomb distortions in EMA reduces the cross section since it goes roughly as q_{eff}^{-4} .

The distortions arising from FSI of an ejected nucleon with the residual nucleus was included in an effective way [25] assuming that the nucleon, propagating as a free particle, sees the energy dependent optical potential V , where V is the average depth of the real part of the optical potential in the region of space in which the initial bound state wave functions are not small ($r < 8$ fm), and as a result carries an effective local momentum p_{eff}

We have used a phenomenological optical potential with significant dependence on the bombarding energy which is a result of the scattering data analysis over a large energy range [26]. The theoretical model to account for this energy-dependence is based on nonlocal quantum exchange effects [27], [28]. Within this model, the nuclear interaction V_N is connected with the folding potential V_F through

$$V_N(R, E) \approx V_F(R) e^{-4v^2/c^2}, \quad (32)$$

where c is the speed of light and v is the local relative speed between the two partners (proton/neutron and residual nucleus), and

$$v^2(R, E) = \frac{2}{\mu} [E - V_C(R) - V_N(R, E)]. \quad (33)$$

The folding potential depends on the densities of the two partners in the collision

$$V_F(R) = \int \rho_1(r_1) \rho_2(r_2) u_0(\vec{R} - \vec{r}_1 + \vec{r}_2) d\vec{r}_1 d\vec{r}_2 . \quad (34)$$

The standard M3Y interaction “frozen” at 10 MeV/nucleon [29] has been assumed for the effective nucleon-nucleon interaction, $u_0(\vec{r})$.

Fig.4 shows the average potential depth ($\langle V_n \rangle$) as a function of the energy for protons (residual nucleus ^{237}Pa) and neutrons (^{237}U). This average depth effectively incorporates distortions connected with FSI and modifies the asymptotic nucleon kinetic energy:

The effect of the optical potential was introduced by replacing the momentum of the ejected nucleon by an effective momentum [25], [30]:

$$p_{eff} = p \sqrt{1 - \frac{\langle V_n \rangle}{T}} , \quad (35)$$

where T is the kinetic energy of the ejected nucleon without FSI. This procedure was included in the Monte Carlo simulations.

We did not take into account distortions arising from a focusing of electron waves and from the imaginary part of the optical potential, since these effects are likely to compensate each other.

VII. DISTORTION CORRECTIONS TO FISSLITY

The fissility P_f for each proton and neutron bound state was calculated without and with the effect of FSI.

In the calculation without FSI we assume that the excitation energy of the doorway states is: $E^* = -E_\alpha + E_F$, where E_α and E_F are the nucleon binding energies for shell α and Fermi level, respectively (see tables 1,2). To estimate the energy deposited by the ejected nucleon in the residual nucleus as a result of the FSI, we assumed that the losses of the nucleon kinetic energy (ΔT), resulting from its passage through the imaginary part of the optical potential, are deposited in the residual nucleus and the excitation energy of the doorway states is $E_{FSI}^* = -E_\alpha + E_F + \Delta T$, where $\Delta T = (1 - \exp(\frac{\langle W \rangle \Delta t}{\hbar})) \frac{T}{2}$, $\langle W \rangle$ is the average depth of the imaginary part of the optical potential, which was taken from

the systematics [31], and Δt is the average nucleon flight time through the imaginary part of the optical potential.

This procedure to take into account the FSI was included in the Monte Carlo simulations. For each fixed transferred ω we choose randomly proton or neutron bound state numbers, and calculate \vec{q} neglecting the recoil energy of the residual nucleus. Then, we generate uniformly the directions of the ejected nucleon with respect to \vec{q} , define the kinetic energy of the outgoing nucleon T , and finally calculate E_{FSI}^* , the corresponding fissility, and the total $(e, e'f)$ -cross section (see Eq.(36))

VIII. FINAL RESULTS

To check how physically reasonable the microscopic-macroscopic approach used for the description of QF fission is, calculations were done with the kinematics conditions of [2], which is the only available experimental data for the reaction under study.

Fig.5 shows the three fold quasi free PWIA cross sections for four proton orbitals of ^{238}U at $\varepsilon_1 = 750$ MeV and $\theta_e = 37.5^\circ$. It is seen that the cross sections show different spectral shapes, which is the result of differences in the momentum distributions for these orbitals. The maxima are shifted with respect to each other according to the differences in the separation energies.

The total (e, e') -cross section is the incoherent sum of the contributions from all proton and neutron orbitals.

Fig.6 shows the total quasi free (e, e') - cross section for $\varepsilon_1 = 750$ MeV and $\theta_e = 37.5^\circ$. The upper part shows the results of the calculations in PWIA, that is, without any corrections arising from the distortions of electron and nucleon waves in the vicinity of the nucleus, while in the lower part the distortions were considered (substitution $q \Rightarrow q_{eff}$, $p \Rightarrow p_{eff}$). The dark circles show the proton contributions, dark triangles - neutron, and light circles- total cross section. The hatched area shows the experimental data [2] after extraction of the Δ resonance peak. It is seen that optical/mean-field distortions

significantly reduce the cross section and slightly shift it to a lower ω . The calculations with distortions qualitatively reproduce the experimental data without any fitting parameters. All parameters used in the calculations were fixed at the microscopic stage.

The differential cross section of the $(e, e'f)$ -reaction was obtained for each proton (p) and neutron (n) bound state α , assuming an isotropic angular distribution for the fission fragments and taking the fissility of the residual nucleus as a factor P_f :

$$\frac{d^5\sigma_{p,n,\alpha}}{d\Omega_e d\varepsilon_2 d\Omega_f}(\varepsilon_2) = \frac{1}{4\pi} \frac{d^3\sigma_{p,n,\alpha}}{d\Omega_e d\varepsilon_2}(\varepsilon_2) P_f \quad (36)$$

The total inclusive quasi free $(e, e'f)$ - cross section was obtained as a sum of proton and neutron contributions:

$$\frac{d^5\sigma_{tot}}{d\Omega_e d\varepsilon_2 d\Omega_f}(\varepsilon_2) = \sum \frac{d^5\sigma_{p,a}}{d\Omega_e d\varepsilon_2 d\Omega_f}(\varepsilon_2) + \sum \frac{d^5\sigma_{n,a}}{d\Omega_e d\varepsilon_2 d\Omega_f}(\varepsilon_2) .$$

Fig. 7 shows the cross section for $\varepsilon_1 = 750$ MeV and $\theta_e = 37.5^\circ$. The upper part shows the calculation in PWIA with distortion corrections to the cross section (by using q_{eff} , p_{eff}), but without correction of the fissility arising from additional excitation (FSI) of the residual nucleus. The lower part shows results similar to the upper part but with FSI corrections to fissility. Light circles in both parts of the fig. 7 show the results of calculations which take into account the preequilibrium emission, dark circles - without accounting of the preequilibrium emission, and the dark triangle with error bars show the experimental data [2]. One sees a strong influence of FSI fissility corrections on the $(e, e'f)$ - cross section, and the calculations with this effect taken into account agree with experimental data. The calculations without and with preequilibrium emission gave close results. Inclusive cross sections are not sensitive to the difference in the reaction mechanisms.

IX. CONCLUSIONS

We presented in this paper a theoretical study of the inclusive quasi free electrofission of ^{238}U . The proton and neutron bound state characteristics were calculated in the framework

of the macroscopic-microscopic approach, using the axially deformed Woods-Saxon single particle potential. The occupation numbers were calculated in the BCS approach. The differential cross sections for the quasi free scattering reaction stage were calculated in PWIA, using off-shell electron-nucleon cross section corrected for Coulomb distortions of electron waves, and FSI distortions for ejected nucleons. The corrected quasi free cross sections reproduce the experimental data fairly well.

The fissility for the single hole states of the residual nuclei was calculated with and without FSI in the framework of two approaches: compound nucleus model without the preequilibrium emission of particles, and the exciton model, which allows for the preequilibrium emission of particles. The account of the FSI corrections to fissility strongly increases it and the calculations agree with available experimental data for the quasi free electrofission of ^{238}U .

The calculations with and without the preequilibrium emission give close results, showing that in inclusive cross sections the effect of preequilibrium emission, averaged over all shells, become small.

In conclusion, the approach based on the microscopic-macroscopic description of nucleon bound states, in conjunction with the plane wave impulse approximation and mean field distortions, give adequate description of inclusive quasi free electrofission at GeV energy range.

X. ACKNOWLEDGMENT

The authors thank the Brazilian agencies CNPq and FAPESP for the partial support to this work, and the graduate student M.S. Vaudeluci for the help in the development of the Monte Carlo code.

REFERENCES

- [1] V.P. Likhachev et al, Contribution of quasielastic scattering to the inclusive electrofission cross section of uranium at $E_0 = 90-250$ MeV, Phys. Rev.C, to be submitted
- [2] K.Hansen et al, Phys.Rev. **C41**(1990)1619.
- [3] T. de Forest, Nucl. Phys. **A392** (1983) 232.
- [4] F. Garcia, O. Rodriguez, J. Mesa, J.D.T. Arruda-Neto, V.P.Likhachev, E. Garrote, R. Capote and F. Guzmán.Comp. Phys. Commun., **120** (1999) 57.
- [5] F. Garcia, E. Garrote, M.-L. Yoneama, J.D.T. Arruda-Neto, J. Mesa, F. Bringas, J.F. Dias, V.P. Likhachev, O. Rodriguez and F. Guzmán, Eur. Phys. J. A **6**, 49 (1999).
- [6] V.M. Strutinsky, Nucl. Phys. **A95**, 420 (1967) .
- [7] V.A. Chepurnov, Sov. J. Nucl. Phys. **6**, 696 (1968).
- [8] F. Garcia, O. Rodriguez, V.A. Rubchenya, E. Garrote, Comp. Phys. Commun. **86** (1995) 129.
- [9] N. Bohr and J. A. Wheeler, Phys. Rev. **56** (1939) 426.
- [10] V. Weisskopf, Phys. Rev. **72** (1947) 1114.
- [11] A.Deppman, O.A.P. Tavares, S.B. Duarte, E.C. de Oliveira, J.D.T.Arruda-Neto, S.R. de Pina, V.P. Likhachev, O. Rodriguez, J.Mesa and M.Goncalves, Phys. Rev. Lett., **87** (2001)182701-1
- [12] A.Deppman, O.A.P. Tavares, S.B. Duarte, E.C. de Oliveira, J.D.T.Arruda-Neto, S.R. de Pina, V.P. Likhachev, O. Rodriguez, J.Mesa and M.Goncalves, Comp. Phys. Commun., in press.
- [13] O. A. P. Tavares and M. L. Terranova, Z. Phys.: Hadr. And Nucl. **343** (1992) 407.
- [14] G. Guaraldo et al., Il Nuovo Cim. **103** (1990) 607.

- [15] R. Vandenbosch and J. R. Huizenga in Nuclear Fission, pp 227, 1^aEd., New York Academic Press, 1973.
- [16] A Gavron et al, Phys.Rev. **C13**, 2374 (1976)
- [17] R.Bonetti, M.B. Chadwick, P. E. Hodgson, B.V. Carlson and M.S. Hussein, Phys. Rep. **202** (1991) 171.
- [18] E.Gadioli and P.E. Hodgson, "Pre-equilibrium Nuclear Reactions " Oxford Univ. Press, 1992.
- [19] J.J. Griffin, Phys. Lett. **17** (1966) 478
- [20] C.K. Cline and M. Blann, Nucl. Phys. **A172** (1972) 225
- [21] G.M. Braga-Marcazzan, E. Gadioli-Erba, L. Millazzo-Colli and P.G. Sona, Phys. Rev. **C6** (1972) 1398
- [22] C. Kalbach, Acta Phys. Slov. **25** (1975) 100
- [23] S.Boffi, C.Giusti and F.D.Pacati, Phys. Reports, **226** (1993) 1
- [24] C.Giusti and F.D.Pacati,Nucl. Phys. **A473** (1987)717
- [25] Kenzo Nakamura and Norihiko Izutsu, Nucl. Phys. **A259** (1976)301
- [26] M. E. Brandan and G. R. Satchler, Phys. Rep. **285** (1992) 142, and references therein.
- [27] L. C. Chamon, D. Pereira and M. S. Hussein, Phys. Rev. **C58** (1998) 576.
- [28] M. A. C. Ribeiro, L. C. Chamon, D. Pereira, M. S. Hussein and D. Galetti, Phys. Rev. Lett. **78** (1997) 3270.
- [29] L. C. Chamon, D. Pereira, M. S. Hussein M. A. C. Ribeiro and D. Galetti, Phys. Rev. Lett. **79** (1997) 5218.
- [30] S. Klavansky, H.W.Kendall, A.K. Kerman and D.Isabelle, Phys.Rev. **C7** (1973) 795

[31] F.D. Becchetti,Jr, and G.W. Greenlees, Phys.Rev. **182** (1969)1190

XI. TABLE 1

| n | [MeV] | πJ | $[N n_z \Lambda]$ | n | [MeV] | πJ | $[N n_z \Lambda]$ | n | [MeV] | πJ | $[N n_z \Lambda]$ |
|----|---------|---------|-------------------|----|---------|---------|-------------------|----|--------|---------|-------------------|
| 1 | -33.685 | 1/2 | 1/2 [0 0 0] | 23 | -16.192 | -3/2 | 3/2 [3 0 1] | 45 | -7.491 | 3/2 | 3/2 [4 0 2] |
| 2 | -31.397 | -1/2 | 1/2 [1 1 0] | 24 | -15.490 | -1/2 | 1/2 [3 0 1] | 46 | -7.195 | 1/2 | 1/2 [4 0 0] |
| 3 | -30.043 | -3/2 | 3/2 [1 0 1] | 25 | -15.415 | 7/2 | 7/2 [4 1 3] | 47 | -6.277 | 5/2 | 5/2 [6 4 2] |
| 4 | -29.670 | -1/2 | 1/2 [1 0 1] | 26 | -14.529 | 9/2 | 9/2 [4 0 4] | 48 | -6.189 | -5/2 | 5/2 [5 2 3] |
| 5 | -28.141 | 1/2 | 1/2 [2 2 0] | 27 | -14.302 | 3/2 | 3/2 [4 2 2] | 49 | -5.348 | -3/2 | 3/2 [5 2 1] |
| 6 | -26.630 | 3/2 | 3/2 [2 1 1] | 28 | -13.984 | -1/2 | 1/2 [5 3 0] | 50 | -4.827 | 7/2 | 7/2 [6 3 3] |
| 7 | -25.963 | 1/2 | 1/2 [2 1 1] | 29 | -13.111 | 1/2 | 1/2 [4 2 0] | 51 | -4.340 | -7/2 | 7/2 [5 1 4] |
| 8 | -25.542 | 5/2 | 5/2 [2 0 2] | 30 | -13.091 | -3/2 | 3/2 [5 4 1] | 52 | -3.949 | -1/2 | 1/2 [5 2 1] |
| 9 | -24.473 | 3/2 | 3/2 [2 0 2] | 31 | -12.383 | 5/2 | 5/2 [4 1 3] | 53 | -3.667 | 1/2 | 1/2 [6 5 1] |
| 10 | -24.025 | -1/2 | 1/2 [3 3 0] | 32 | -11.735 | -5/2 | 5/2 [5 3 2] | 54 | -3.465 | -5/2 | 5/2 [5 1 2] |
| 11 | -22.836 | 1/2 | 1/2 [2 0 0] | 33 | -11.053 | 7/2 | 7/2 [4 0 4] | 55 | -3.417 | 9/2 | 9/2 [6 2 4] |
| 12 | -22.716 | -3/2 | 3/2 [3 2 1] | 34 | -10.831 | 3/2 | 3/2 [4 1 1] | 56 | -3.051 | -9/2 | 9/2 [5 0 5] |
| 13 | -21.614 | -1/2 | 1/2 [3 2 1] | 35 | -10.388 | -1/2 | 1/2 [5 4 1] | 57 | -2.261 | 11/2 | 11/2 [6 1 5] |
| 14 | -21.292 | -5/2 | 5/2 [3 1 2] | 36 | -10.280 | -7/2 | 7/2 [5 2 3] | 58 | -2.207 | -1/2 | 1/2 [7 5 0] |
| 15 | -20.333 | -7/2 | 7/2 [3 0 3] | 37 | -9.794 | 1/2 | 1/2 [4 1 1] | 59 | -2.182 | 7/2 | 7/2 [5 0 3] |
| 16 | -19.621 | -3/2 | 3/2 [3 1 2] | 38 | -9.301 | 5/2 | 5/2 [4 0 2] | 60 | -1.773 | 3/2 | 3/2 [6 4 2] |
| 17 | -19.254 | 1/2 | 1/2 [4 2 0] | 39 | -9.054 | -9/2 | 9/2 [5 1 4] | 61 | -1.669 | 1/2 | 1/2 [6 4 0] |
| 18 | -18.229 | -5/2 | 5/2 [3 0 3] | 40 | -8.356 | -3/2 | 3/2 [5 3 2] | 62 | -1.553 | -3/2 | 3/2 [7 4 1] |
| 19 | -18.189 | 3/2 | 3/2 [4 3 1] | 41 | -8.276 | 1/2 | 1/2 [6 4 0] | 63 | -1.459 | 13/2 | 13/2 [6 0 6] |
| 20 | -18.130 | -1/2 | 1/2 [3 1 0] | 42 | -8.217 | -11/2 | 11/2 [5 0 5] | 64 | -1.118 | -3/2 | 3/2 [5 1 2] |
| 21 | -16.730 | 5/2 | 5/2 [4 2 2] | 43 | -7.624 | -1/2 | 1/2 [5 3 0] | 65 | -1.065 | -1/2 | 1/2 [5 1 0] |
| 22 | -16.416 | 1/2 | 1/2 [4 3 1] | 44 | -7.597 | 3/2 | 3/2 [6 5 1] | 66 | -0.393 | -5/2 | 5/2 [7 5 2] |

XII. TABLE 2

| n | [MeV] | πJ | $\Omega[N n_z \Lambda]$ | n | [MeV] | πJ | $\Omega[N n_z \Lambda]$ | n | [MeV] | πJ | $\Omega[N n_z \Lambda]$ |
|----|----------|---------|-------------------------|----|----------|---------|-------------------------|----|----------|---------|-------------------------|
| 1 | -42.0542 | 1/2 | 1/2 [0 0 0] | 31 | -19.7288 | -3/2 | 3/2 [5 4 1] | 61 | -9.3350 | 1/2 | 1/2 [6 4 0] |
| 2 | -39.0049 | -1/2 | 1/2 [1 1 0] | 32 | -18.9901 | 7/2 | 7/2 [4 0 4] | 62 | -9.20000 | 11/2 | 11/2 [6 1 5] |
| 3 | -37.9568 | 3/2 | 3/2 [1 0 1] | 33 | -18.9635 | 3/2 | 3/2 [4 1 1] | 63 | -8.6428 | -1/2 | 1/2 [7 5 0] |
| 4 | -37.6894 | -1/2 | 1/2 [1 0 1] | 34 | -18.4784 | -5/2 | 5/2 [5 3 2] | 64 | 8.4314 | 13/2 | 13/2 [6 0 6] |
| 5 | -35.3282 | 1/2 | 1/2 [2 2 0] | 35 | -18.1710 | 1/2 | 1/2 [4 1 1] | 65 | -8.3129 | -3/2 | 3/2 [5 0 1] |
| 6 | -34.0676 | 3/2 | 3/2 [2 1 1] | 36 | -17.7626 | -1/2 | 1/2 [5 4 1] | 66 | -8.2710 | -5/2 | 5/2 [5 0 3] |
| 7 | -33.5860 | 1/2 | 1/2 [2 1 1] | 37 | -17.6098 | 5/2 | 5/2 [4 0 2] | 67 | -7.9719 | -3/2 | 3/2 [7 6 1] |
| 8 | -33.1312 | 5/2 | 5/2 [2 0 2] | 38 | -17.1797 | -7/2 | 7/2 [5 2 3] | 68 | -7.6257 | -1/2 | 1/2 [5 0 1] |
| 9 | -32.3233 | 3/2 | 3/2 [3 2 1] | 39 | -16.2814 | 3/2 | 3/2 [4 0 2] | 69 | -7.4628 | 5/2 | 5/2 [6 3 3] |
| 10 | -31.2577 | 1/2 | 1/2 [2 0 0] | 40 | -16.0693 | -9/2 | 9/2 [5 1 4] | 70 | -7.4347 | 3/2 | 3/2 [6 3 1] |
| 11 | -30.9731 | -1/2 | 1/2 [3 3 0] | 41 | -15.9987 | 1/2 | 1/2 [4 0 0] | 71 | -6.8936 | -5/2 | 5/2 [7 5 2] |
| 12 | -29.7758 | -3/2 | 3/2 [3 2 1] | 42 | -15.9048 | -3/2 | 3/2 [5 3 2] | 72 | -6.1818 | 1/2 | 1/2 [6 3 1] |
| 13 | -28.9791 | -1/2 | 1/2 [3 2 1] | 43 | -15.3084 | -1/2 | 1/2 [5 3 0] | 73 | -5.6980 | -5/2 | 5/2 [6 2 2] |
| 14 | -28.5603 | -5/2 | 5/2 [3 1 2] | 44 | -15.2725 | -11/2 | 11/2 [5 0 5] | 74 | -5.5954 | -7/2 | 7/2 [7 4 3] |
| 15 | -27.6884 | -7/2 | 7/2 [3 0 3] | 45 | -14.7923 | 1/2 | 1/2 [6 4 0] | 75 | -5.5815 | 7/2 | 7/2 [6 2 4] |
| 16 | -27.2878 | -3/2 | 3/2 [3 1 2] | 46 | -14.0318 | 3/2 | 3/2 [6 5 1] | 76 | -4.4142 | -1/2 | 1/2 [7 7 0] |
| 17 | -26.2258 | -1/2 | 1/2 [3 1 0] | 47 | -14.0081 | -5/2 | 5/2 [5 2 3] | 77 | -4.3051 | 7/2 | 7/2 [6 1 3] |
| 18 | -26.0583 | -5/2 | 5/2 [3 0 3] | 48 | -13.2796 | -3/2 | 3/2 [5 2 1] | 78 | -4.2459 | -9/2 | 9/2 [7 3 4] |
| 19 | -26.0283 | 1/2 | 1/2 [4 4 0] | 49 | -12.8670 | 5/2 | 5/2 [6 4 2] | 79 | -4.0132 | 9/2 | 9/2 [6 1 5] |
| 20 | -24.9930 | 3/2 | 3/2 [4 3 1] | 50 | -12.3859 | -7/2 | 7/2 [5 1 4] | 80 | -3.9400 | 1/2 | 1/2 [6 2 0] |
| 21 | -24.5673 | -3/2 | 3/2 [3 0 1] | 51 | -12.2367 | -1/2 | 1/2 [5 2 1] | 81 | -3.7016 | 3/2 | 3/2 [6 2 2] |
| 22 | -24.0164 | -1/2 | 1/2 [3 0 1] | 52 | -11.6318 | -5/2 | 5/2 [5 1 2] | 82 | -3.3495 | 9/2 | 9/2 [6 0 4] |

| | | | | | | | | | | | |
|----|----------|------|--------------|----|----------|------|--------------|----|---------|-------|---------------|
| 23 | -23.7133 | 1/2 | 1/2 [4 3 1] | 53 | -11.5394 | 7/2 | 7/2 [6 3 3] | 83 | -3.0797 | -1/2 | 1/2 [7 6 0] |
| 24 | -23.7025 | 5/2 | 5/2 [4 2 2] | 54 | -11.2224 | 1/2 | 1/2 [6 5 1] | 84 | -3.0058 | -11/2 | 11/2 [7 2 5] |
| 25 | -22.5412 | 7/2 | 7/2 [4 0 4] | 55 | -11.2192 | -9/2 | 9/2 [5 0 5] | 85 | -2.8563 | 11/2 | 11/2 [6 0 6] |
| 26 | -21.8511 | 3/2 | 3/2 [4 2 2] | 56 | 10.4881 | -7/2 | 7/2 [5 0 3] | 86 | -2.6835 | -3/2 | 3/2 [7 6 2] |
| 27 | -21.7120 | 9/2 | 9/2 [4 0 4] | 57 | -10.2634 | 9/2 | 9/2 [6 2 4] | 87 | -2.3053 | 3/2 | 3/2 [6 1 1] |
| 28 | -20.9447 | 1/2 | 1/2 [4 2 0] | 58 | -9.8951 | -3/2 | 3/2 [5 1 2] | 88 | -2.2208 | 1/2 | 1/2 [8 6 0] |
| 29 | -20.6103 | -1/2 | 1/2 [5 5 0] | 59 | -9.8517 | -1/2 | 1/2 [5 1 0] | 89 | -1.9882 | -13/2 | 13/2 [7 1 6] |
| 30 | -20.1878 | 5/2 | 5/2 [4 1 3] | 60 | -9.4457 | 3/2 | 3/2 [6 4 2] | 90 | -1.8461 | 5/2 | 5/2 [6 1 3] |

XIII. FIGURE CAPTIONS

Fig.1. Occupation probabilities for the single particle bound states of ^{238}U . Upper part corresponds to protons, lower to neutrons.

Fig.2. Typical momentum distribution for proton bound states.

Fig.3. Fissility for ^{237}Pa and $^{237,238}\text{U}$. The solid (dotted) curve shows the results of calculations on the statistical approach without (with) account of preequilibrium particle emission. The dark strips show the experimental data (see text for details).

Fig.4. Average real potential depth as a function of the nucleon energy. The dashed curve corresponds to protons (residual nucleus ^{237}Pa); solid curve to neutrons (^{237}U).

Fig.5. PWIA quasi free (e, e') – cross section for four proton orbitals of ^{238}U and $\varepsilon_1 = 750$ MeV, $\theta_e = 37.5^\circ$. The dark triangles correspond to $n=1$ (see table 1), light triangles to $n=11$, light circles to $n=21$, and dark circles to $n=31$.

Fig.6. Quasi free (e, e') –cross section for $\varepsilon_1 = 750$ MeV and $\theta_e = 37.5^\circ$. The upper part shows the results of calculations in PWIA, lower -with account of distortion corrections (see text for details) . The dark circles show the proton contribution, dark triangles - neutron, and light circles - total cross section. The hatched area represents the experimental data [2]

Fig. 7. Total quasi free $(e, e'f)$ –cross section for $\varepsilon_1 = 750$ MeV and $\theta_e = 37.5^\circ$. The upper part shows the calculation in PWIA with account of distortion corrections to the cross section, but without account of FSI corrections to the fissility (see text for details). The lower part shows results similar to the upper part, but with account of FSI corrections to the fissility. The light circles show the results of calculations which take into account the preequilibrium emission, and dark circles - without accounting of the preequilibrium emission. The dark triangle with error bars represents the experimental data [2]

XIV. TABLE CAPTION

Table 1. Proton single-particle levels of ^{238}U . The Fermi level is the level 46.

Table 2. Neutron single-particle levels of ^{238}U . The Fermi level is the level 73.

Fig.1

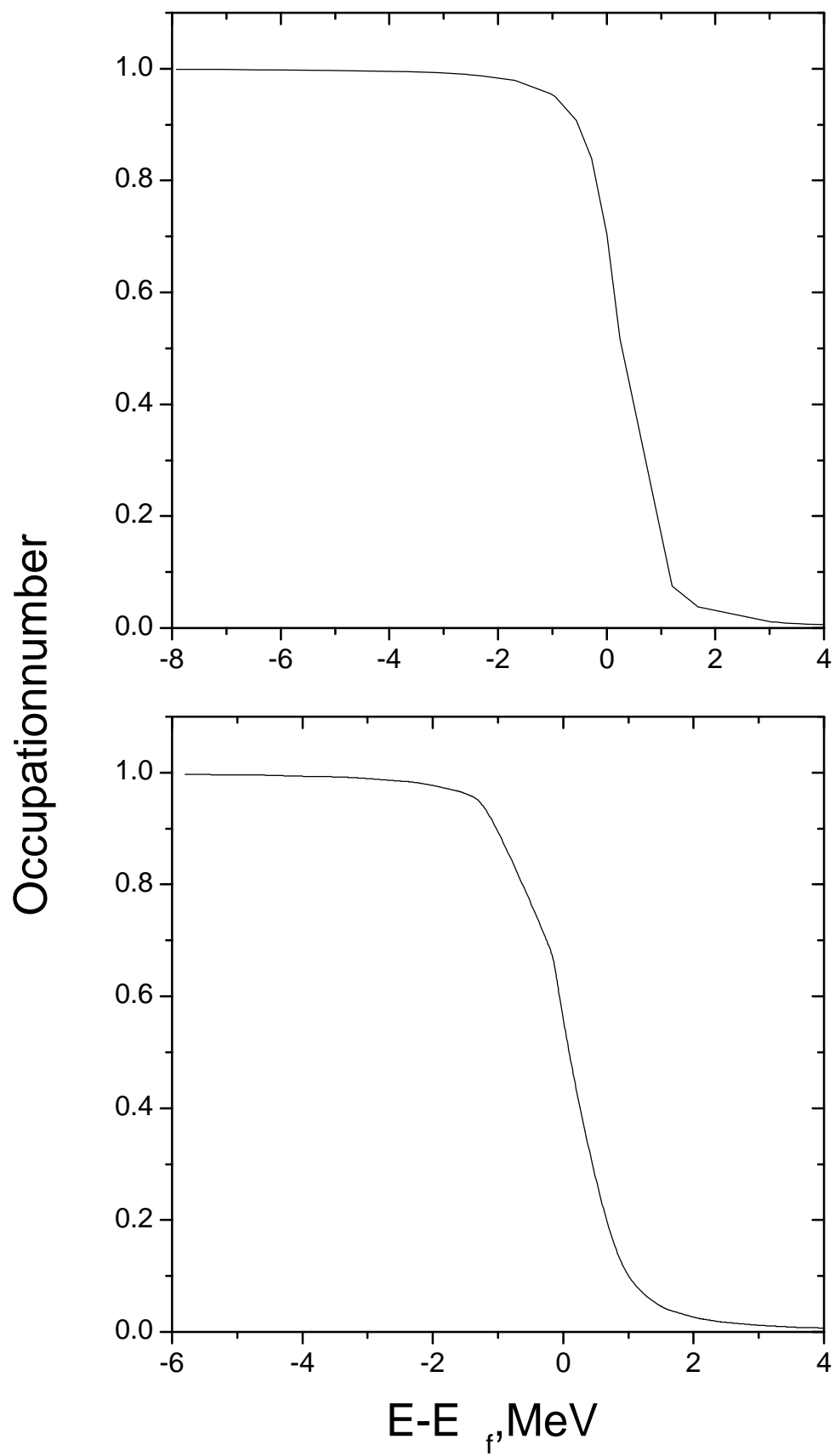


Fig.2

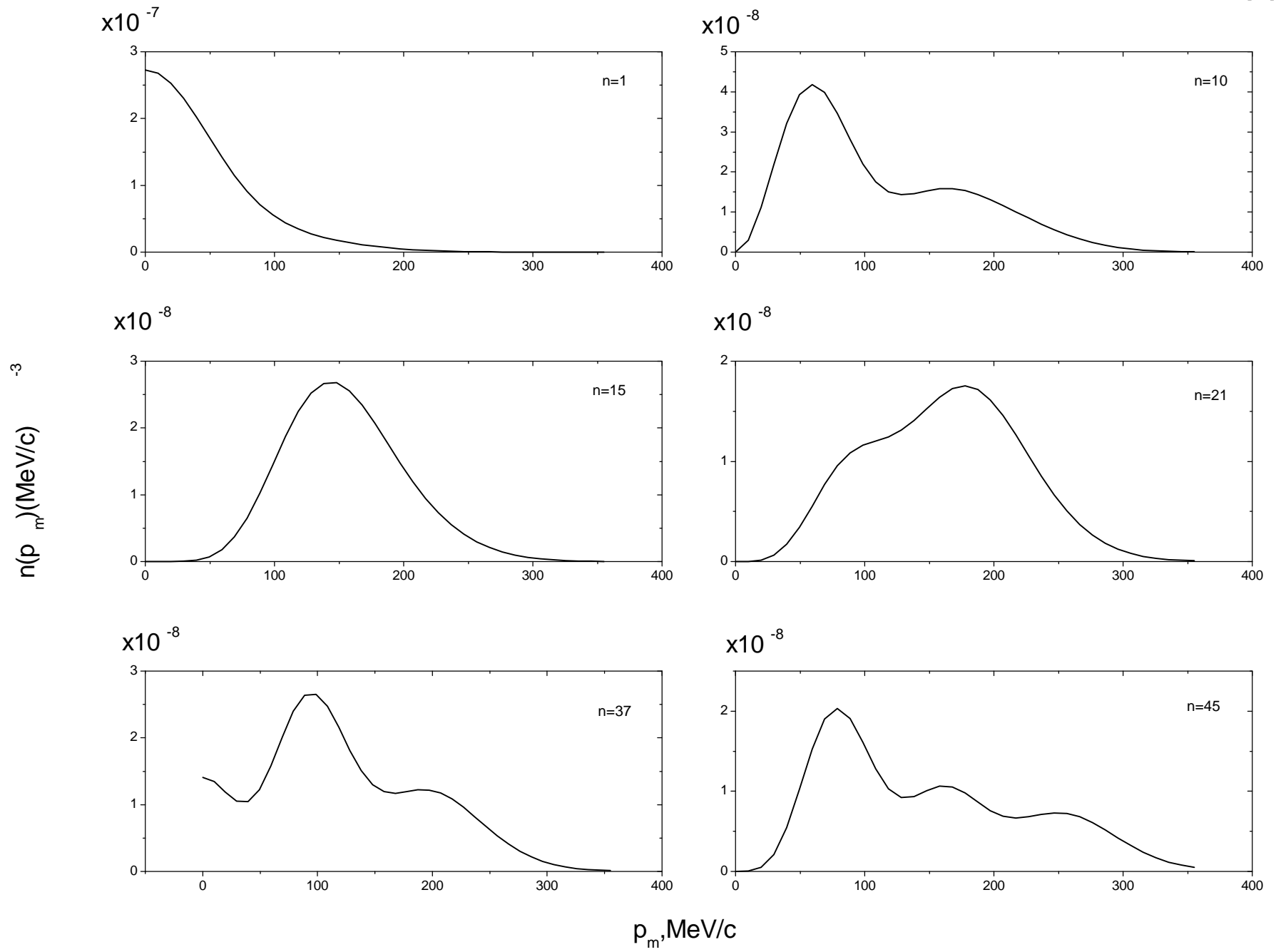


Fig.3

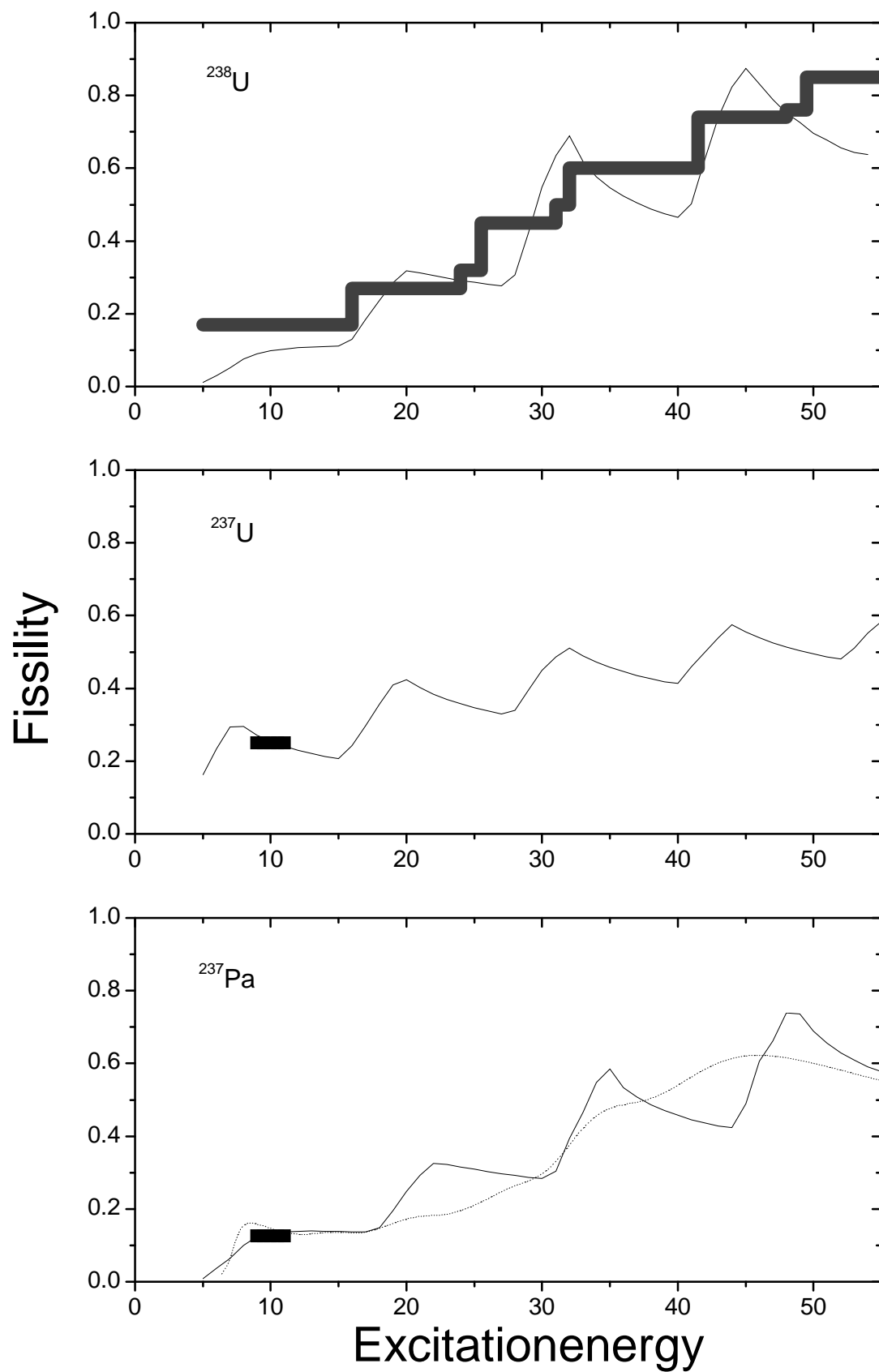


Fig.4

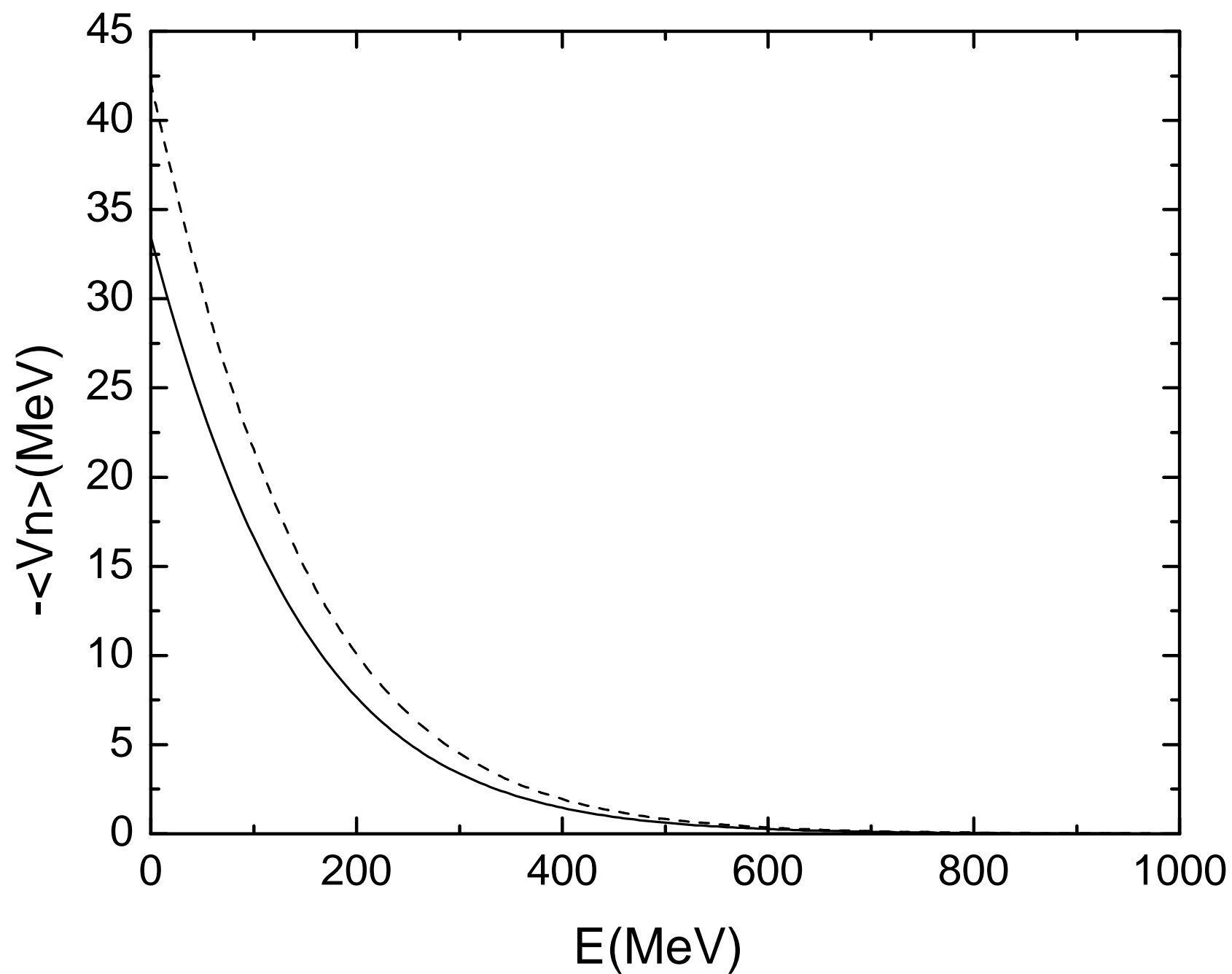


Fig.5

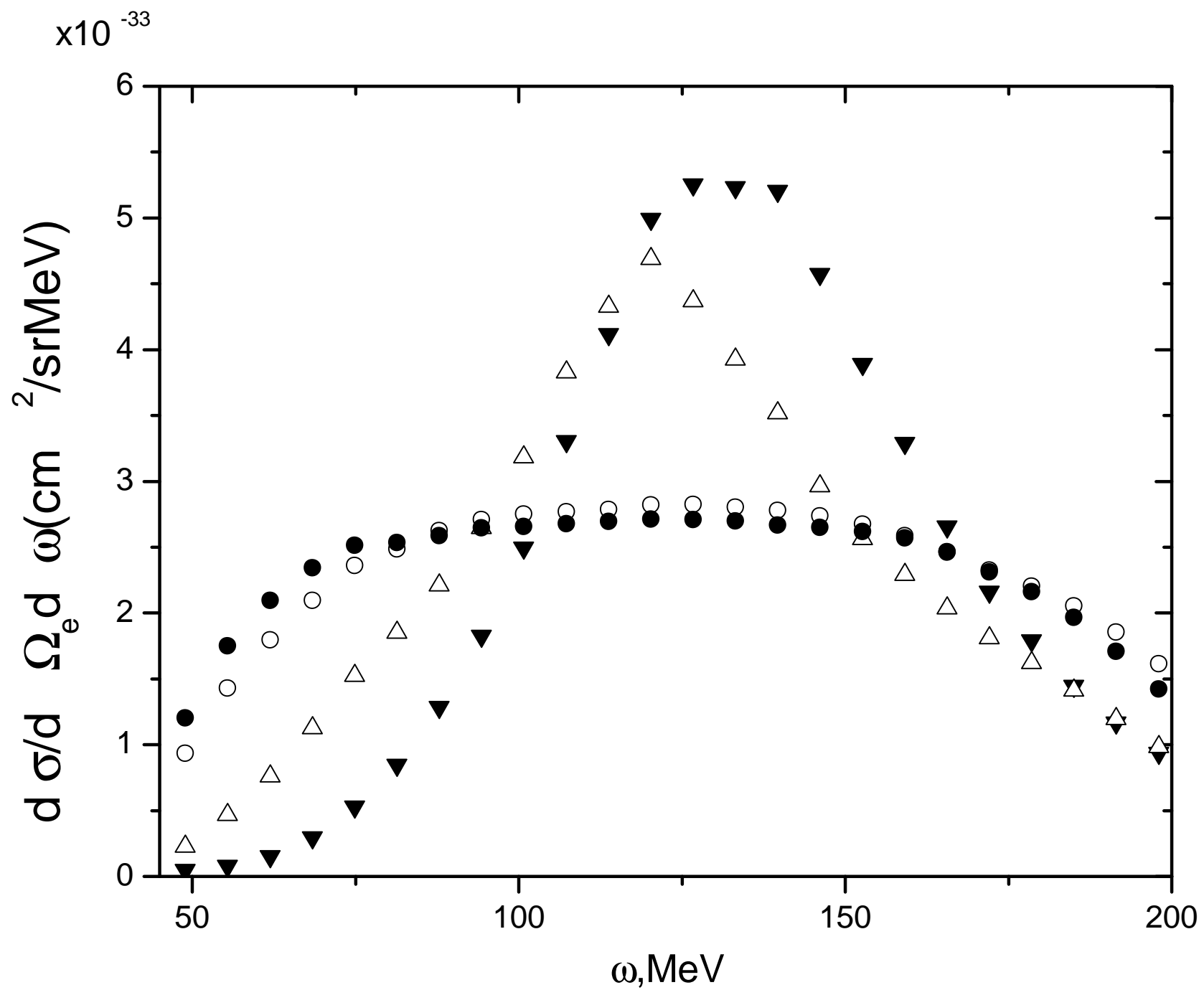


Fig.6

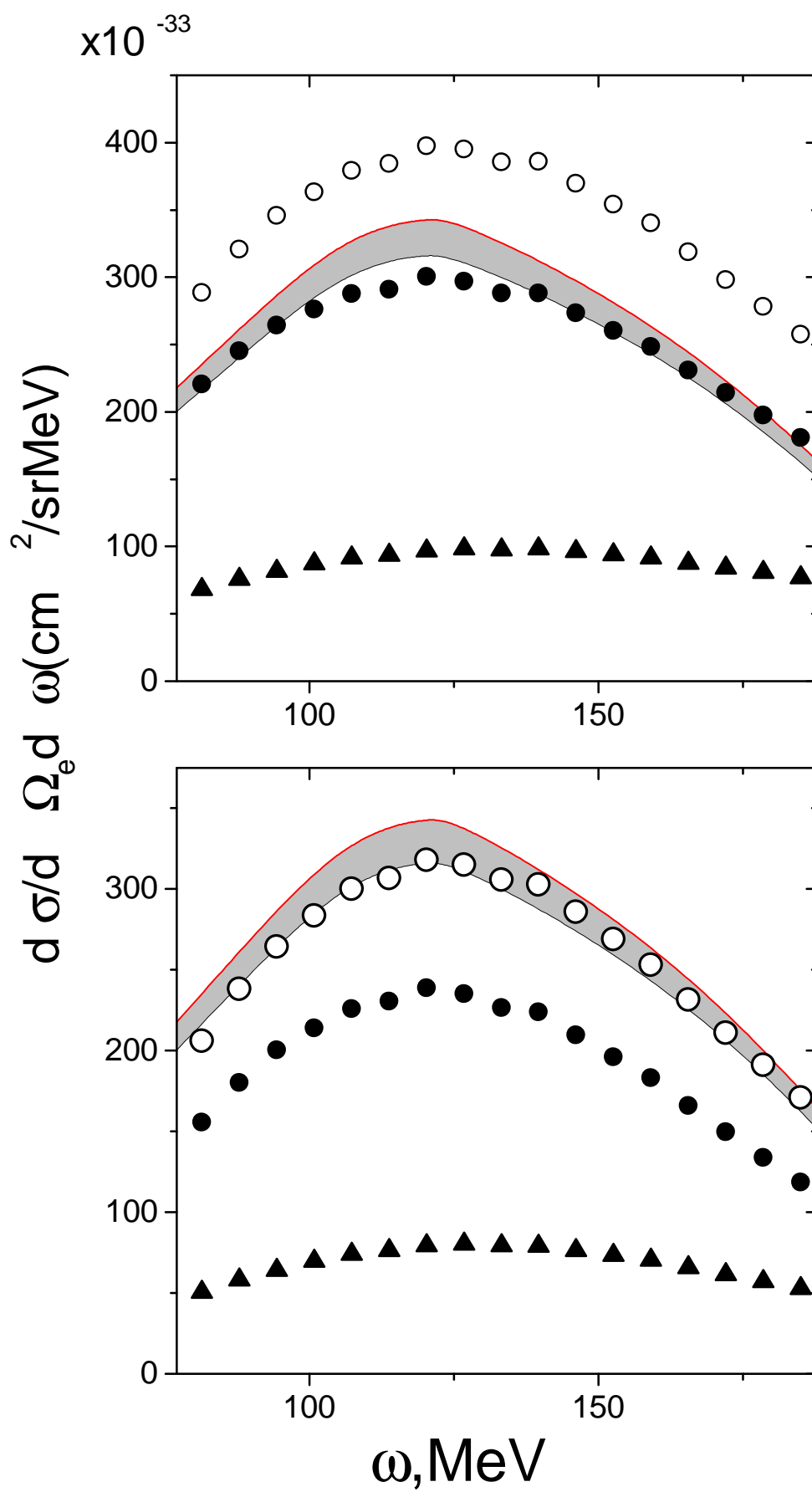


Fig.7

